Theor Chim Acta (1993) 86: 115–127

Theoretica Chimica Acta

A spherically averaged representation of the atomic one-particle reduced density matrix

Hartmut Schmider and Vedene H. Smith, Jr.
Department of Chemistry, Queen's University, Kingston K7L 3N6, Ontario, Canada

Received July 1, 1992/Accepted September 23, 1992

Summary. A new way of representing the one-particle reduced density matrix (ODM) of closed-shell atoms in a spherically averaged manner is presented, and connections of this representation to the radial density distribution $D(R)$ and the isotropic reciprocal form factor $B(s)$ are shown. In this representation, certain characteristics of the angular nodal structure of the natural orbitals (NOs) are preserved. Examples of hydrogenic orbitals and near-Hartree–Fock wave functions for some closed-shell atoms are given.

Key words: One-particle reduced density matrix – Closed-shell atoms

1 Introduction

Among the great revelations in Löwdin's 1955 series of papers [1] were the properties of the one-particle reduced density matrix (ODM) [2] and the introduction of its eigenfunctions, the natural spin-orbitals. The *spin-traced* ODM (in the following simply denoted as ODM) includes, as is well known, all information about the *spin-independent* one-particle properties of the system. Its connection to various experimentally obtainable quantities are well documented in the literature [3].

However, graphical representations of the ODM have only been given sparsely [4–7], which can be explained by the fact, that $\varrho(\vec{r}, \vec{r}')$ is a function of six variables (three for each of the coordinates $\vec{r}$ and $\vec{r}'$), and that therefore some process of reducing the number of independent variables has to be applied. For atomic systems, the natural means by which to do this is a spherical-averaging procedure.

Recently, Gadre et al. [6] have published contour-plots of spherically averaged $\varrho(\vec{r}, \vec{r}')$ for some closed-shell atoms of the first three rows of the periodic table. They obtain these by equating the polar and azimuthal angles (Θ, ϕ) and (Θ', ϕ') and integrating over the resulting 'angular cut' through ϱ:

$$\varrho(r, r') = \frac{1}{4\pi} \int\int \varrho(\vec{r}, \vec{r}')|_{\Theta' = \Theta, \phi' = \phi} \sin\Theta \, d\Theta \, d\phi. \tag{1}$$

This procedure does not account for the off-diagonal of the angular part of ϱ (i.e. $\Theta' \neq \Theta$ and $\phi' \neq \phi$, respectively), and therefore does not preserve informa-

tion about the angular nodal structure of the natural orbitals $\phi(\vec{r})$ (NOs; these are the eigenfunctions of the spin-traced ODM; its eigenvalues are the associated occupation numbers n_i [1].)

$$\varrho(\vec{r}, \vec{r}') = \sum_i n_i \phi_i(\vec{r}) \phi_i^*(\vec{r}'). \tag{2}$$

The procedure we propose in the present paper replaces the combination of a 'cut' $(\Theta', \phi') = (\Theta, \phi)$ and a two-dimensional spherical integration by a four-dimensional integration over angles. As will be shown, these integrations preserve information about the angular nodes of the NOs as well as certain connections of the ODM to one-particle properties.

2 The ODM and certain one-particle properties

As is well known [1], the diagonal of the ODM ($\vec{r}' = \vec{r}$) is the charge density of the electronic system under consideration:

$$\varrho(\vec{r}) = \varrho(\vec{r}, \vec{r}). \tag{3}$$

The off-diagonal parts of $\varrho(\vec{r}, \vec{r}')$ bear no direct relationship to $\varrho(\vec{r})$, but are connected indirectly with the corresponding momentum density $\Pi(\vec{p})$. This connection is established via the so-called reciprocal form factor (or internally folded density) [8–11] $B(\vec{s})$. $B(\vec{s})$ is given as an internal convolution of the ODM or an autocorrelation function of its natural orbitals [8, 10]:

$$B(\vec{s}) = \int \varrho(\vec{r}, \vec{r} + \vec{s})\, d\vec{r} = \sum_i n_i \int \phi_i(\vec{r}) \phi_i^*(\vec{r} + \vec{s})\, d\vec{r}. \tag{4}$$

The natural orbitals are denoted by ϕ_i, and the n_i stand for the eigenvalues of the ODM, the occupation numbers.

$B(\vec{s})$ is also, by the convolution theorem of Fourier transforms, the three-dimensional Fourier transform of the momentum density $\Pi(\vec{p})$ [8]:

$$B(\vec{s}) = \int e^{-i\vec{s}\cdot\vec{p}} \Pi(\vec{p})\, d\vec{p}. \tag{5}$$

This connection of the off-diagonal of the ODM with the momentum density makes the whole $\varrho(\vec{r}, \vec{r}')$ an interesting subject of investigation.

It is not trivial to preserve this relationship with momentum-space properties in the course of a reduction of the number of independent variables in ϱ. For an atomic system, for example, one cannot calculate the isotropic reciprocal form factor

$$B(s) = \frac{1}{4\pi} \int\int B(\vec{s})\, d\Omega_s,$$
$$d\Omega_s = \sin\Theta_s\, d\Theta_s\, d\phi_s. \tag{6}$$

by a direct integration of the form (4) over the spherically averaged ODM of the form of Eq. (1):

$$B(s) \neq \int \varrho(r, r+s) r^2\, dr, \tag{7}$$

since in the construction of $\varrho(r, r')$ the implicit assumption that $\vec{r}'$ be parallel to $\vec{r}$ has been made.

To obtain a representation of the ODM, where a simpler integration of the form of Eq. (4) yields $B(s)$, we will change the coordinate system.

3 The ODM in extracular and intracular coordinates

The ODM $\varrho(\vec{r}, \vec{r}')$ may easily be transformed into another set of coordinates given by:

$$\vec{R} = \frac{(\vec{r} + \vec{r}')}{2}, \tag{8}$$

$$\vec{s} = \vec{r}' - \vec{r}, \tag{9}$$

which are called extracular and intracular coordinates, respectively [12–15]. The nomenclature of the different vectors and angles involved is given in Fig. 1. In our case, we can write:

$$\tilde{\varrho}(\vec{R}, \vec{s}) = \varrho(\vec{r}, \vec{r}'). \tag{10}$$

This corresponds to a transformation of the positions $\vec{r}$ and $\vec{r}'$ into 'center-of-mass' coordinates. The Jacobian of the transformation is unity.

The resulting representation $\tilde{\varrho}$ of the ODM should not be confused with the so-called intracule and extracule matrices which are the result of the same coordinate transformation on the second-order reduced density matrix Γ_2 (see e.g. [13]). In the latter case the transformation is applied to the pair of coordinates $\vec{r}_1$ and $\vec{r}_2$ ($\vec{r}'_1$ and $\vec{r}'_2$, respectively), which correspond to *two different* particles, not the *same* particle as in the former.

The connections to the charge density $\varrho(\vec{R})$ and the internally folded density $B(\vec{s})$ take the form:

$$\varrho(\vec{R}) = \tilde{\varrho}(\vec{R}, 0) \tag{11}$$

and

$$B(\vec{s}) = \int \tilde{\varrho}(\vec{R}, \vec{s})\, d\vec{R} \tag{12}$$

in this coordinate system.

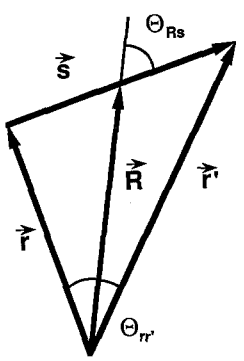

Fig. 1. Extracular and intracular coordinates used in this work. Since the polar axis may be chosen to coincide with $\vec{R}$, $\Theta_{rr'}$ is the difference in the polar angles of $\vec{r}'$ and $\vec{r}$

A spherical-averaging procedure can now be readily applied to this representation of the ODM by integrating over the angular part of the extracular coordinate $\vec{R}$.

$$\bar{\tilde{\varrho}}(R, \vec{s}) = \frac{1}{4\pi} \int\int \tilde{\varrho}(\vec{R}, \vec{s})\, d\Omega_R. \tag{13}$$

This is, in the case of a spherically symmetric closed-shell atom, trivial, since the ODM does not depend on the *absolute* orientation of the pair of vectors $\vec{r}$ and $\vec{r}'$. Note, that we do not restrict ourselves by requiring that $\Theta_R = \Theta_s$. We only average over all directions of the 'center-of-mass' of $\vec{r}$ and $\vec{r}'$.

The second spherical average is now performed over the angle between the $\vec{R}$ and the $\vec{s}$ vectors, i.e. over the possible orientations of the line of interconnection between $\vec{r}$ and $\vec{r}'$.

$$\bar{\bar{\tilde{\varrho}}}(R, s) = \frac{1}{4\pi} \int\int \bar{\tilde{\varrho}}(R, \vec{s})\, d\Omega_{Rs}. \tag{14}$$

The ϕ_{Rs} integration is again trivial for closed-shell atoms, since the value of the ODM does (because of the spherical symmetry) not depend on the azimuthal angle between $\vec{R}$ and $\vec{s}$. The Θ_{Rs} integration, however, has to be performed explicitly.

As can be seen in Fig. 1, the lengths of $\vec{r}$ and $\vec{r}'$, as well as the angle $\Theta_{rr'}$ between them, are functions of $\vec{R}$, $\vec{s}$ and Θ_{Rs}:

$$r = \sqrt{R^2 + \left(\frac{s}{2}\right)^2 - Rs\cos\Theta_{Rs}},$$

$$r' = \sqrt{R^2 + \left(\frac{s}{2}\right)^2 + Rs\cos\Theta_{Rs}},$$

$$\cos(\Theta_{rr'}) = \frac{r^2 + r'^2 - s^2}{2rr'} = \frac{R^2 - \left(\frac{s}{2}\right)^2}{\sqrt{\left(R^2 + \left(\frac{s}{2}\right)^2\right)^2 - R^2 s^2 \cos^2\Theta_{Rs}}}. \tag{15}$$

The ODM $\varrho(\vec{r}, \vec{r}')$ will depend on the angle $\Theta_{rr'}$, if it has eigenfunctions with angular quantum numbers $l > 0$. For a *complete* subshell of orbitals with angular quantum number l, the dependency of ϱ on $\Theta_{rr'}$ takes the form of a Legendre Polynomial of order l:

$$\sum_{m=-l}^{l} Y_l^m{}^*(\Theta', \phi') Y_l^m(\Theta, \phi) = \frac{2l+1}{4\pi} P_l(\cos\Theta_{rr'}). \tag{16}$$

For the examples in the next section, the Θ_{Rs} integration was performed numerically, employing an algorithm described by Patterson [16].

We could now proceed to examine the function $\bar{\bar{\tilde{\varrho}}}(R, s)$, since it has the interesting properties:

$$\varrho(R) = \bar{\bar{\tilde{\varrho}}}(R, 0) \tag{17}$$

and

$$B(s) = 4\pi \int \bar{\bar{\tilde{\rho}}}(R, s) R^2\, dR, \tag{18}$$

where $\varrho(R)$ is the spherically averaged charge density and $B(s)$ is the isotropic reciprocal form factor. We choose to weight the resulting spherically averaged ODM $\bar{\bar{\varrho}}$ by a factor of $4\pi R^2$, in order to arrive at the representation:

$$\varrho^{\Omega}(R, s) = 4\pi R^2 \bar{\bar{\varrho}}(R, s) = \frac{R^2}{4\pi} \int\int\int\int \tilde{\varrho}(\vec{R}, \vec{s})\, d\Omega_R\, d\Omega_{Rs}, \tag{19}$$

in which case Eqs. (17) and (18) become:

$$D(R) = \varrho^{\Omega}(R, 0) \tag{20}$$

and

$$B(s) = \int \varrho^{\Omega}(R, s)\, dR. \tag{21}$$

Here $D(R)$ denotes the well-known radial density distribution:

$$D(R) = 4\pi R^2 \varrho(R) = R^2 \int\int \varrho(\vec{R})\, d\Omega_R. \tag{22}$$

Equations (20) and (21) are somewhat simpler than their equivalents of Eqs. (17) and (18). Equation (21) shows, that the connection between the momentum space quantity $B(\vec{s})$ and the off-diagonal of the ODM has been conserved in the spherical-averaging procedure. Note also, that ϱ^{Ω} still includes information about the angular nodal structure of the constituting natural orbitals via Eqs. (15) and (16), whereas the spherically averaged ODM $\varrho(r, r')$ (see Eq. (1)) does not.

4 Some examples: Hydrogenic orbitals and closed-shell atoms

In order to demonstrate the general features of ϱ^{Ω}, Figs. 2–7 show contour plots of this function for some hydrogenic orbitals ($Z = 1$). Note that for $l > 0$, the plots represent full subshells of $2l + 1$ orbitals with magnetic quantum numbers $-l \leqslant m \leqslant l$. To facilitate comparison, all functions have been normalized to $\int D(R)\, dR = \int \varrho^{\Omega}(R, 0)\, dR = 1$.

As one can easily see, the radial nodes of the $2s$ and $3s$ orbitals show up along the R-axis as zeros in $D(R)$ and in the 'off-diagonal' region ($s > 0$) as closed nodal loops. Note, that the off-diagonal exhibits at least n negative areas for an ns-orbital, since each zero in $D(R)$ splits up into one of the afore-mentioned loops. It is interesting that, by integration, negative areas lead to a local lowering of $B(s)$, which may result in wiggles, shoulders or (in the case of atoms with p-occupation) even negative values [10] of this function, corresponding to the overlap of regions of opposite sign in the orbital (see Eq. (4)).

All s-orbitals exhibit slight wiggles along the line $R = s/2$, which may be explained by the fact, that for these (R, s) values, the maximum at the nucleus enters the calculation of the spherical average (at $|\cos(\Theta_{Rs})| = 1$).

The orbital-subshells with higher angular quantum numbers ($l > 0$) show nodal lines, which extend from the origin to the off-diagonal. Their total number equals l.

For orbitals with odd l one of these lines may always be assigned to $R = s/2$ or $\cos \Theta_{rr'} = 0$, and therefore the (odd-order) Legendre polynomial in Eq. (16) vanishes identically over the range of the Θ_{Rs} integration. For the other nodal lines, no such simple relationship exists, since the value of the Legendre polynomial

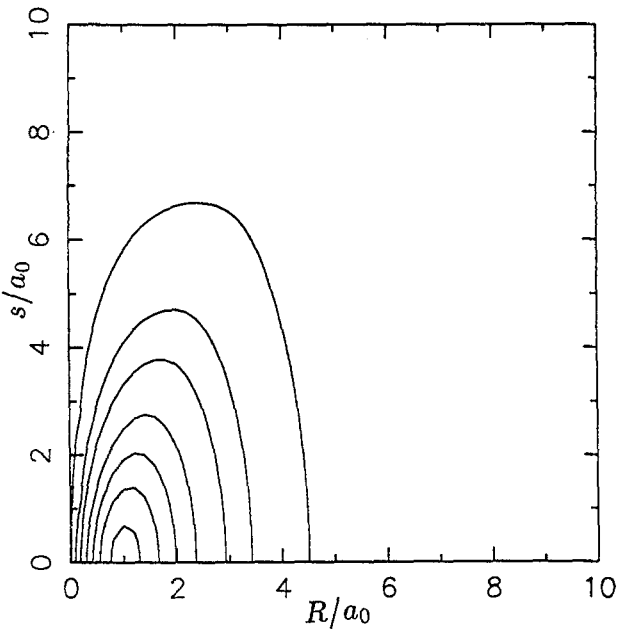

Fig. 2. ϱ^{Ω} for the 1*s* hydrogenic orbital. *Contour lines* are shown for 0.01, 0.05, 0.1, 0.2, 0.3, 0.4 and $0.5e^{-}/a_0$. The orbital is normalized to $1e^{-}$

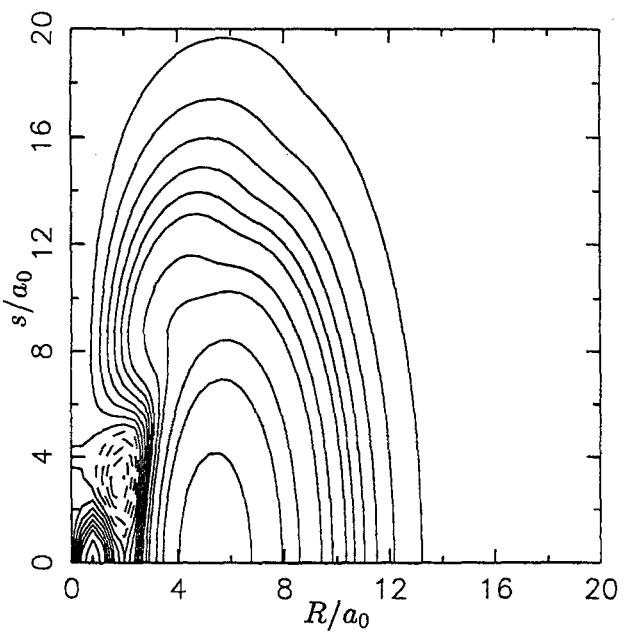

Fig. 3. ϱ^{Ω} for the 2*s* hydrogenic orbital. Non-negative contours are *full*, negative ones are *dashed*. *Contour lines* are shown for −0.025, −0.02, −0.015, −0.01, −0.005, 0.0, 0.005, 0.01, 0.015, 0.02, 0.025, 0.03, 0.04, 0.05, 0.075, 0.1 and $0.15e^{-}/a_0$. The orbital is normalized to $1e^{-}$

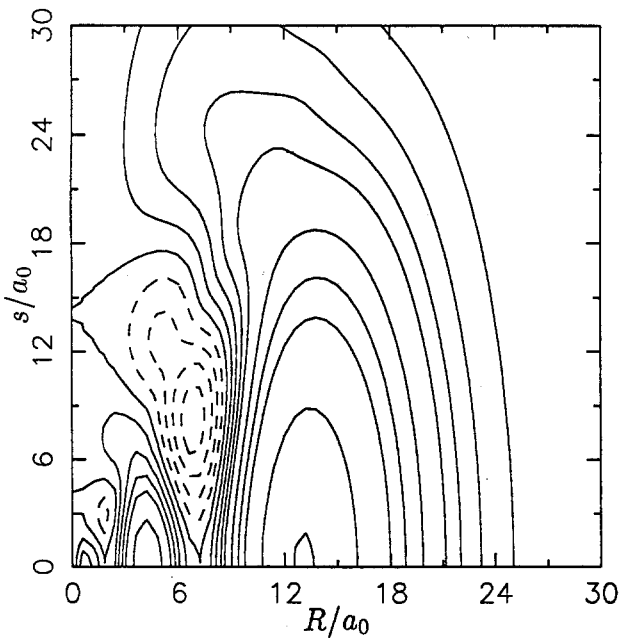

Fig. 4. ϱ^{Ω} for the 3*s* hydrogenic orbital. Non-negative contours are *full*, negative ones are *dashed. Contour lines* are shown for −0.02, −0.015, −0.01, −0.005, 0.0, 0.005, 0.01, 0.015, 0.02, 0.03, 0.04, 0.05, 0.075 and $0.1e^{-}/a_0$. The orbital is normalized to $1e^{-}$

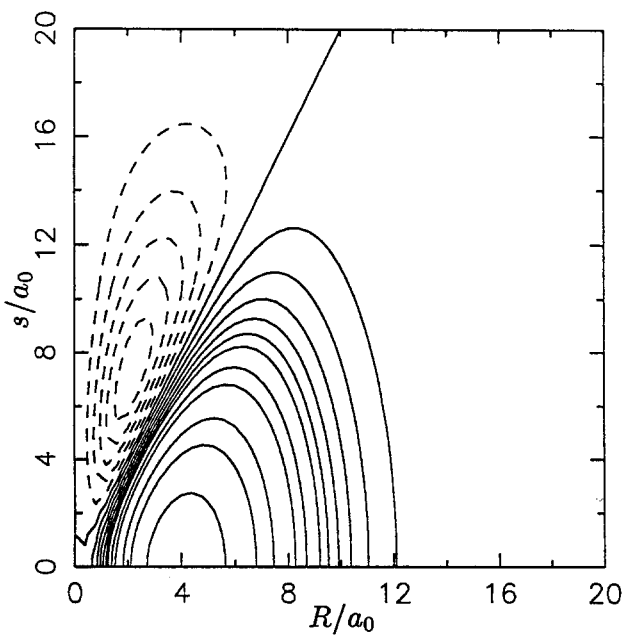

Fig. 5. ϱ^{Ω} for a set of 2*p* hydrogenic orbitals. Non-negative contours are *full*, negative ones are *dashed. Contour lines* shown are for −0.025, −0.02, −0.015, −0.01, −0.005, 0.0, 0.005, 0.01, 0.015, 0.02, 0.025, 0.03, 0.04, 0.05, 0.075 0.1 and $0.15e^{-}/a_0$. The set is normalized to $1e^{-}$

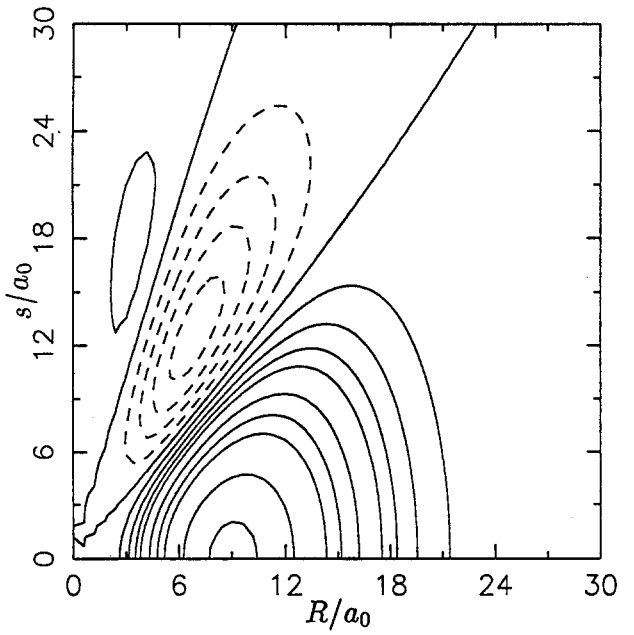

Fig. 6. ϱ^{Ω} for a set of $3d$ hydrogenic orbitals. Non-negative contours are *full*, negative ones are *dashed*. *Contour lines* shown are for -0.02, -0.015, -0.01, -0.005, 0.0, 0.005, 0.01, 0.015, 0.02, 0.03, 0.04, 0.05, 0.075 and $0.1e^{-}/a_0$. The set is normalized to $1e^{-}$

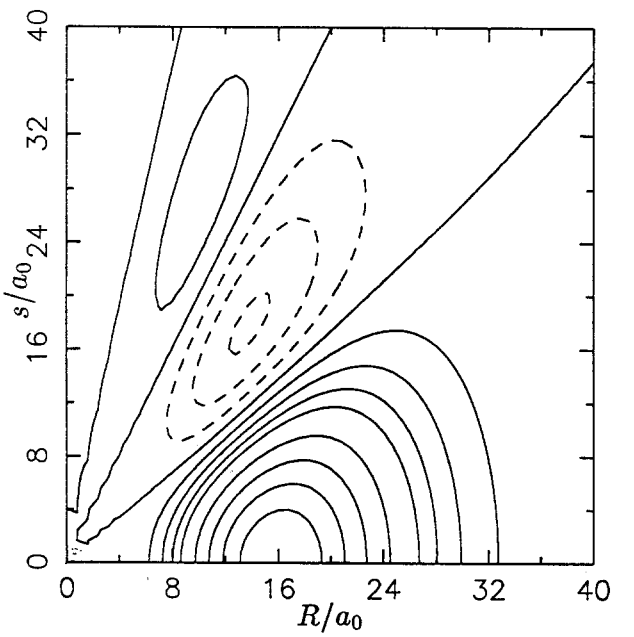

Fig. 7. ϱ^{Ω} for a set of $4f$ hydrogenic orbitals. Non-negative contours are *full*, negative ones are *dashed*. *Contour lines* shown are for -0.015, -0.01, -0.005, 0.0, 0.005, 0.01, 0.015, 0.02, 0.03, 0.04, 0.05 and $0.06e^{-}/a_0$. The set is normalized to $1e^{-}$

remains dependent on the integration variable $\cos(\Theta_{Rs})$. As a result, an integral equation has to be solved to determine the roots of ϱ^{Ω}.

To estimate the position of these nodal lines, we consider first a case where the exponential in the (r, r') radial part of the integrand is independent of the angle Θ_{Rs}. This would be the situation for (spherical harmonic) Gaussian type orbitals (GTOs) [17]. Then the expression inside the Θ_{Rs} integral reduces to a polynomial in R^2 and $(s/2)^2$ and the roots of the resulting analytic function may be found explicitly.

For a set of $2p$-GTOs this yields (as mentioned previously):

$$R = s/2. \tag{23}$$

For a set of $3d$-GTOs one obtains:

$$R = \frac{s}{2}\sqrt{3} \quad \text{and} \quad R = \frac{s}{2}\frac{1}{\sqrt{3}}, \tag{24}$$

and for the $4f$-case the result is:

$$R = (s/2), \qquad R = \frac{s}{2}\sqrt{3+\sqrt{8}} \quad \text{and} \quad R = \frac{s}{2}\sqrt{3-\sqrt{8}}. \tag{25}$$

For the physically more relevant Slater-type functions, such as the ones used throughout this work, the actual position of the nodal lines are quite similar to the ones above. How strongly they deviate depends on how strongly the exponential $e^{-Z(r+r')}$ is Θ_{Rs} dependent, i.e. on its anisotropy in intracular/extracular coordinates. The STO nodal curves do not even have to be (and for all cases other than the previously mentioned $R = s/2$ are not) straight lines.

The total ϱ^{Ω} of an atomic system will, of course, be a superposition of the contributions from each of its natural orbitals, weighted by the corresponding occupation numbers n_i. We have computed and plotted ϱ^{Ω} for some closed-shell atoms of the first and third rows of the periodic table, using the near-HF wave functions of Clementi and Roetti [18], which are given in an optimized STO basis set. The contour plots for Be, Ne, Ca, and Zn are shown in Figs. 8–11. An extension to open-shell systems would require the assumption of a statistical mixture of possible degenerate configurations to give a spherically symmetric total or the treatment of the totally symmetric component of the ODM [19].

For the beryllium atom (Fig. 8), the most prominent feature of ϱ^{Ω} is the distinction between the K and L shells. The influence of the minimum in the radial density $D(R)$ which may be used to define this shell boundary [20, 21], extends well into the off-diagonal region of ϱ^{Ω} and leads to a valley separating the main areas of domination by the $1s$ and $2s$ contribution. No negative areas are visible so that negative values for the reciprocal form factor $B(s)$ cannot be expected. $B(s)$ of beryllium is indeed positive definite.

The neon atom (Fig. 9) shows a different topology in ϱ^{Ω}. There is still a minimum in $D(R)$, separating the core from the valence region. The valley extending from this minimum is strongly modified by the influence of the nodal line, which is the consequence of the p-occupation in neon. For small values of R and s it is bent, but approaches for higher values the line $R = s/2$, as may be expected from the considerations for $2p$ orbitals above.

These two basic patterns are repeated in the following atoms with an increasing complexity. As an example might serve calcium (Fig. 10), where the negative area in ϱ^{Ω} is mainly due to p-contributions. The zero line deviates very strongly from linearity. This is due to the overwhelming influence of the diffuse $4s$ orbital which extends over quite a large region of R and s.

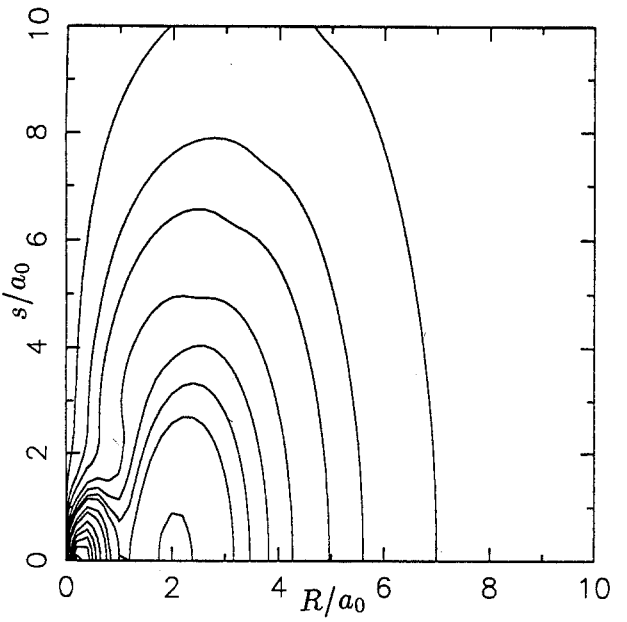

Fig. 8. ϱ^{Ω} for the beryllium atom in the NHF approximation. Contour lines shown are for 0.01, 0.05, 0.1, 0.2, 0.3, 0.4, 0.5, 0.75, 1.0, 1.5, 2.0, 2.5, 3.0 and $3.5e^{-}/a_0$.

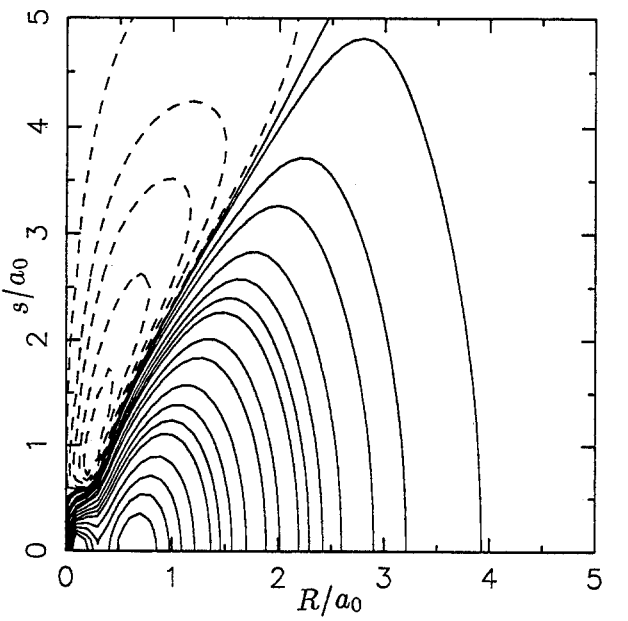

Fig. 9. ϱ^{Ω} for the neon atom in the NHF approximation. Non-negative contours are *full*, negative ones are *dashed*. *Contour lines* shown are for -0.3, -0.2, -0.1, -0.05, -0.01, 0.0, 0.01, 0.05, 0.1, 0.2, 0.3, 0.4, 0.5, 0.75, 1.0, 1.5, 2.0, 2.5, 3.0, 4.0, 5.0, 6.0 and $7.0e^{-}/a_0$

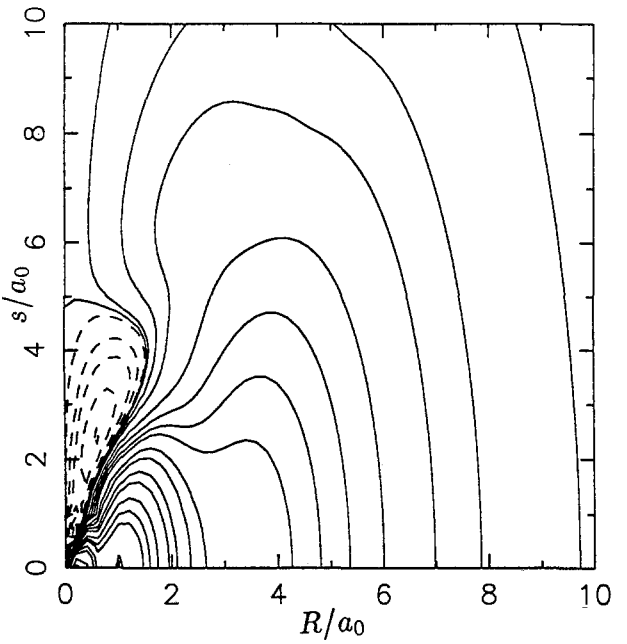

Fig. 10. ϱ^{Ω} for the calcium atom in the NHF approximation. Non-negative contours are *full*, negative ones are *dashed. Contour lines* shown are for -0.6, -0.5, -0.4, -0.3, -0.2, -0.1, -0.05, -0.01, 0.0, 0.01, 0.05, 0.1, 0.2, 0.3, 0.4, 0.5, 0.75, 1.0, 1.5, 2.0, 3.0, 4.0, 5.0, 7.5, 10.0, 15.0 and $20.0e^{-}/a_0$

Zinc (Fig. 11) serves as a last example, to demonstrate the influence of a closed d-shell on the topography of the spherically averaged ODM. Since d-orbitals show two nodal lines we expect two positive areas in ϱ^{Ω}, separated by a negative one (as in Fig. 6). This feature is actually found, but it is strongly modified by the influence of the $4s$-orbital which joins the two regions for larger (R, s). The result is a 'pond' in the ODM. The impact of p-contributions to the total is fairly difficult to estimate since their nodal line crosses this pond and only modifies its shape. For this atom, we have included graphs of $D(R)$ and $B(s)$ in Fig. 11 in order to indicate the respective functions obtained from a cut at $s = 0$ (Eq. (20)) and an integration over R (Eq. (21)).

5 Conclusions and outlook

We have demonstrated for the examples of several hydrogenic orbitals and closed-shell atoms, that the ODM of a spherically symmetric system may be represented by a function of only two *radial* variables R and s in such a way, that important *angular* features are retained. This representation, which is based on the transformation into intra- and extracular coordinates, shows a simple and direct connection (Eq. (20)) with the radial density $D(R)$. It also preserves the integral relation (Eq. (4)) with the Fourier transform of the momentum density, $B(s)$, that holds generally for the anisotropic ODM of electronic systems.

Information about contributions of orbitals with different angular behaviour may be extracted from the corresponding contour plots by inspection. In the case

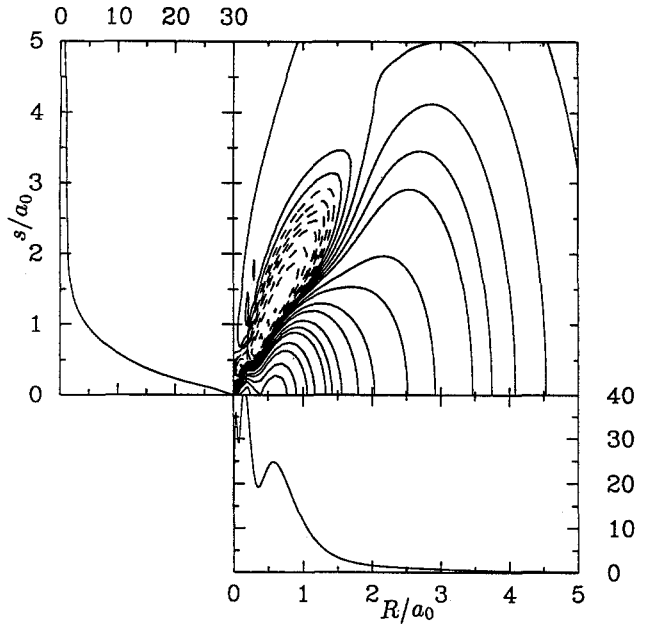

Fig. 11. ϱ^{Ω} for the zinc atom in the NHF approximation. Non-negative contours are *full*, negative ones are *dashed*. *Contour lines* shown are for -1.5, -1.0, -0.75, -0.5, -0.4, -0.3, -0.2, -0.1, -0.05, -0.01, 0.0, 0.01, 0.05, 0.1, 0.2, 0.3, 0.4, 0.5, 0.75, 1.0, 1.5, 2.0, 3.0, 4.0, 5.0, 7.5, 10.0, 15.0, 20.0 and $30.0e^{-}/a_0$. At the bottom, the radial charge distribution $D(R)$ is shown to indicate the cut through ϱ^{Ω} at $s = 0$. The curve at the left shows $B(s)$, i.e. the integral $\int \varrho^{\Omega}(R, s)\, dR$

of single orbital contributions, it is possible to infer the orbital type by counting the radial and angular nodes in the ODM. This feature is not found in the conventional representation (Eq. (1)).

The restriction to closed-shell systems need not be retained if one is only interested in the statistical mixture of degenerate ground-states of atoms or in the totally symmetric component of the ODM.

An extension to the momentum space representation of the ODM, namely $\varrho(\vec{p}, \vec{p}')$ is straightforward, since the angular part of the natural orbitals is retained in the course of a Fourier transformation [22]. Only the radial part of the matrix changes from an exponential-type to a Lorentzian-type behaviour. For non-zero l quantum numbers, additional modifications of the radial part occur [22]. The connections (Eqs. (20) and (21)) have clearly their counterparts in momentum space, namely:

$$I(P) = \varrho_M^{\Omega}(P, 0) \tag{26}$$

and

$$F(k) = \int \varrho_M^{\Omega}(P, k)\, dP, \tag{27}$$

where P and k are the equivalents of R and s. Here, the radial momentum density $I(P) = 4\pi P^2 \Pi(P)$ and the coherent form factor $F(k)$ take the place of $D(R)$ and $B(s)$, respectively. ϱ_M^{Ω} denotes the ODM in an analogous representation in momentum space. Given the importance of the momentum density and

reciprocal space quantities such as $F(k)$, an investigation of this representation of the ODM is well worthwhile and is presently being carried out in this laboratory.

Acknowledgments. This research has been financed by grants from NSERCC (Natural Science and Engineering Council of Canada). H.S. gratefully acknowledges an Ontario Graduate Scholarship (OGS).

References

1. Löwdin PO (1955) Phys Rev 97:1490
2. Husimi K (1940) Proc Phys Math Soc Japan 22:264, This introduction of reduced density matrices went, for the obvious reasons, unnoticed in the West
3. Smith VH, Jr (1980) in: Becker P (ed) Electron and magnetization densities in molecules and crystals. Plenum Press, NY, p 3 and references therein
4. Sperber G (1971) Int J Quantum Chem 5:189
5. Weyrich W (1988) Lecture given at the Sagamore IX Conf on Charge, Spin and Momentum Densities, Workshop on Density Matrices, Coimbra, Portugal
6. Gadre SR, Kulkarni SA, Pathak RK (1989) Phys Rev A 40:4224
7. Schmider H, Edgecombe KE, Smith VH, Jr, Weyrich W (1992) J Chem Phys 96:8411
8. Benesch R, Singh SR, Smith VH, Jr (1971) Chem Phys Lett 10:151
9. Weyrich W, Pattison P (1979) Chem Phys 41:271
10. Weyrich W (1979) Habilitationsschrift, Darmstadt
11. Thakkar AJ, Simas AM, Smith VH, Jr (1981) Chem Phys 63:271
12. Thakkar AJ, Tanner AC, Smith VH, Jr (1987) in: Erdahl R, Smith VH, Jr (eds) Density matrices and density functionals. D Reidel, Amsterdam, p 327
13. Thakar AJ (1987) in: Erdahl R, Smith VH, Jr (eds) Density matrices and density functionals. D Reidel, Amsterdam, p 553
14. Eddington AS (1946) Fundamental theory. Cambridge Univ Press p 19
15. Coleman AJ (1967) Int J Quantum Chem Symp 1:457
16. Patterson TNL (1968) Math Comp 22:847, See also NAG-Fortran library, Mark 12 (1986), program D01AHF. The obvious choice of a Gauss–Legendre quadrature for this kind of problem is plagued with convergence problems. We resorted to a more reliable, albeit somewhat slower quadrature
17. Harris FE (1963) Rev Mod Phys 35:558
18. Clementi E, Roetti C (1974) Atom Data Nucl Data Tables 14:177
19. Kutzelnigg W, Smith VH, Jr (1968) Int J Quantum Chem 2:531
20. Politzer P, Parr RG (1976) J Chem Phys 64:4634
31. Simas AM, Sagar RP, Ku ACT, Smith VH, Jr (1988) Can J Chem 66:1923
22. Kaijser P, Smith VH, Jr (1977) Adv Quantum Chem 10:37